

New structural model for GeO_2/Ge interface: A first-principles study

Shoichiro Saito* and Tomoya Ono

Graduate School of Engineering, Osaka University

(Dated: March 28, 2011)

Abstract

First-principles modeling of a $\text{GeO}_2/\text{Ge}(001)$ interface reveals that sixfold GeO_2 , which is derived from cristobalite and is different from rutile, dramatically reduces the lattice mismatch at the interface and is much more stable than the conventional fourfold interface. Since the grain boundary between fourfold and sixfold GeO_2 is unstable, sixfold GeO_2 forms a large grain at the interface. On the contrary, a comparative study with SiO_2 demonstrates that SiO_2 maintains a fourfold structure. The sixfold GeO_2/Ge interface is shown to be a consequence of the ground-state phase of GeO_2 . In addition, the electronic structure calculation reveals that sixfold GeO_2 at the interface shifts the valence band maximum far from the interface toward the conduction band.

PACS numbers: 68.35.-p, 77.55.dj, 61.50.Ks

* saito@cp.prec.eng.osaka-u.ac.jp

With the continued scaling of Si metal-oxide-semiconductor (MOS) devices, it is becoming increasingly difficult to enhance device performance; therefore, new channel materials have been explored. Ge is considered as one of the best channel materials for obtaining high performance MOS devices due to its higher carrier mobility. The narrower band gap of Ge is also attractive since lower operation voltage lowers energy consumption. To fabricate high performance devices with a Ge channel, one of the most crucial challenges is fabricating an insulator with superior interface properties since the termination of the surface states is important for device reliability. So far, various insulators have been examined, for example, GeO_2 [1, 2], Ge_3N_4 [3], and high- k oxides [4–6]. Among these insulators, GeO_2 is the most fundamental and important, similar to SiO_2 in Si MOS technology, because it exists even in high- k oxide/Ge interfaces. A considerable number of studies have been conducted on the process of developing high quality GeO_2/Ge interfaces, and several groups have reported that GeO_2/Ge interfaces, fabricated by conventional dry oxidation, have a low interface trap density (mid 10^{10} – 10^{11} $\text{cm}^{-2}\text{eV}^{-1}$) [1, 2]. Houssa *et al.* simulated the density of Ge dangling bonds at the GeO_2/Ge interface as a function of the oxidation temperature, by combining viscoelastic data of GeO_2 and the modified Maxwell’s model, and claimed that the density of Ge dangling bonds is less than that of Si dangling bonds at the SiO_2/Si interface [7]. Their results are in good agreement with other reported results [1, 2].

Interface stress between a semiconductor and an oxide is considered as one of the origins of interface defects. Kageshima and Shiraishi predicted that Si atoms are emitted from the interface to release stress induced by the lattice-constant mismatch between SiO_2 and Si, although the dangling bonds remain after Si atom emission [8]. On the other hand, we calculated the probability of Ge atom emission from a GeO_2/Ge interface by using the interface model proposed by Kageshima and Shiraishi and found that hardly any Ge atoms are emitted from the GeO_2/Ge interface [9]. We concluded that the flexibility of the O-Ge-O bonds contributes to the relaxation of interface stress, resulting in a GeO_2/Ge interface that is superior to the SiO_2/Si one. Watanabe *et al.* claimed, using the classical molecular-dynamics simulation, that the narrow equilibrium Ge-O-Ge bond angles contribute to the reduction in compressive stress in GeO_2 films as well as flexible O-Ge-O bonds [10]. Although a considerable number of first-principles studies on the GeO_2/Ge interface have been conducted based on the calculations on SiO_2/Si interfaces [7, 11–15], the atomic and electronic structures of the GeO_2/Ge interface have not been identified experimentally because GeO_2 is both

water-soluble and thermally unstable at elevated temperatures.

We propose a complete ordered $\text{GeO}_2/\text{Ge}(001)$ interface structure with minimum lattice mismatch. Our interface model consists of sixfold GeO_2 , which is derived from cristobalite and is different from rutile, on a $\text{Ge}(001)$ substrate. The sixfold GeO_2/Ge interface is more stable by 1.92 eV than the conventional fourfold GeO_2/Ge interface. The lattice mismatch between sixfold GeO_2 and Ge ($\sim 5\%$) is much smaller than that between fourfold GeO_2 and Ge ($\sim 17\%$). By examining a mixed fourfold and sixfold GeO_2/Ge interface model, we find that sixfold GeO_2 exists as a large grain at the GeO_2/Ge interface. On the contrary, SiO_2 at the SiO_2/Si interface maintains a fourfold structure. A comparative study of the electronic structures of the sixfold and fourfold GeO_2/Ge interfaces shows that the valence band maximum (VBM) far from the interface varies due to the existence of sixfold GeO_2 at the interface.

Our first-principles calculation method is based on the real-space finite-difference approach [16–18], which enables us to determine a self-consistent electronic ground state with a high degree of accuracy using a timesaving double-grid technique [17, 18]. The norm-conserving pseudopotentials [19] of Troullier and Martins [20] are used to describe the electron-ion interaction and are transformed into the computationally efficient Kleinman-Bylander separable form [21], using the s and p components as nonlocal components for H, O, and Si, and the s , p , and d components as nonlocal components for Ge. Exchange and correlation effects are treated using the local density approximation [22]. The coarse grid spacing of ~ 0.13 Å, which corresponds to the plane wave cutoff energy of ~ 112 Ry, is used for all of our calculations. We first examine the atomic structures of GeO_2 and SiO_2 bulks in the cristobalite phases ($c\text{-GeO}_2$ and $c\text{-SiO}_2$) under pressure along the a -axis because these structures correspond to the directions parallel to the interface when the oxides are piled on the (001) surface. The $c\text{-GeO}_2$ ($c\text{-SiO}_2$) structure is tetragonal with four GeO_2 (SiO_2) molecules per unit cell, and $4 \times 4 \times 3$ k -point grids in the Brillouin zone are taken into account. The $c\text{-GeO}_2$ structure at the equilibrium point is shown in Fig. 1(a). The equilibrium lattice parameters of $c\text{-GeO}_2$ and $c\text{-SiO}_2$, which are obtained from first-principles calculation, are listed in Table I. We then compress $c\text{-GeO}_2$ ($c\text{-SiO}_2$) along the a -axis by 5-25 (5-35)% from the equilibrium lattice constants and optimize the length of the c -axis in increments of 1% to determine the energy minima. We relax all the atoms until all the force components drop below 0.05 eV/Å.

65 Figures 2(a) and 2(b) show the total energies of c -GeO₂ and c -SiO₂ per molecular unit
 66 as a function of volume. The energy minima of other phases [quartz (\square), cristobalite (\circ),
 67 and rutile (\triangle)] without any constraints are also depicted for comparison. The zero on the
 68 energy scale is the rutile structure of GeO₂ and the quartz structure of SiO₂. In this figure,
 69 the c -GeO₂ at about $0.78a_0^{\text{GeO}_2}$ shows a local minimum, where $a_0^{\text{GeO}_2}$ represents the length of
 70 the a -axis of c -GeO₂ at the equilibrium point (4.818 Å). The atomic structure of the strained
 71 c -GeO₂ at the local minimum is shown in Fig. 1(b). The c -GeO₂ under a certain pressure
 72 transforms into a sixfold structure, which is distinct from the rutile phase, by rotating oxygen
 73 atoms around the Ge atoms. The energy minimum of sixfold GeO₂ is lower than that of
 74 fourfold GeO₂ since the zero-temperature phase of GeO₂ has a sixfold rutile structure. The
 75 critical point between the fourfold and sixfold structures is about $0.85a_0^{\text{GeO}_2}$. The arrow on
 76 the upper horizontal axis corresponds to the lateral length of the Ge(001)-(1×1) surface. It
 77 should be noted that GeO₂ forms a sixfold structure when the length of the a -axis is equal
 78 to that of the (1×1) surface, while the c -SiO₂ still maintains a fourfold structure.

79 We next compare the energetic stability of the sixfold GeO₂/Ge(001) interface with the
 80 fourfold one since the lattice mismatch between the sixfold GeO₂ and Ge(001) surfaces is
 81 small ($\sim 5\%$). Figures 3(a) and 3(b) show the fourfold and sixfold GeO₂/Ge interfaces,
 82 respectively. The fourfold oxide transforms into a sixfold one by rotating the four oxygen
 83 atoms around one Ge atom in a Ge(001)-(1×1) surface unit. The total energy difference
 84 between the fourfold and sixfold SiO₂/Si interfaces are also calculated for comparison. The
 85 Ge(001)-($\sqrt{2} \times \sqrt{2}$) surface is used for the lateral size of the supercell of the GeO₂/Ge
 86 interface, and the length of the supercell perpendicular to the surface is $5.5a_0^{\text{Ge}}$, where a_0^{Ge} is
 87 the optimized lattice constant of the Ge bulk (5.578 Å). The model of the interface includes
 88 seven Ge atomic and two GeO₂ molecular layers, and both sides of the surface are simply
 89 terminated with H atoms. Eight k -points in the 1×1 lateral unit cell are used for the
 90 Brillouin zone sampling. All the atoms, except the Ge atoms in the bottom-most layer
 91 and the H atoms terminating their dangling bonds, are relaxed. The other computational
 92 details are the same as those used in the bulk calculation. We found that the sixfold GeO₂/Ge
 93 interface is more stable by 1.92 eV than the fourfold one because the interface stress between
 94 GeO₂ and Ge is released by the phase transition into the dense sixfold structure. On the
 95 other hand, the fourfold c -SiO₂/Si interface model is preferable by 1.02 eV compared with
 96 the sixfold one. Kageshima and Shiraishi reported that Si atoms at the c -SiO₂/Si interface

are emitted to release interface stress, resulting in a quartz-SiO₂/Si interface [8]. On the other hand, hardly any Ge atoms at the *c*-GeO₂/Ge interface are emitted [9]. Our results indicate that the sixfold structure contributes to the release of interface stress due to the lattice mismatch between the *c*-GeO₂ and Ge(001) surfaces.

Since the lateral length of the Ge(001)-(1×1) surface is longer than that of the sixfold GeO₂ surface but shorter than that of the fourfold *c*-GeO₂ surface in Fig. 2(a), there is a possibility that *c*-GeO₂ on the Ge(001) surface is composed of a mixed fourfold and sixfold structure. We examine the total energies of the supercell doubling of the Ge(001)-($\sqrt{2} \times \sqrt{2}$) surface unit in the two directions, i.e., the supercell contains eight Ge(001)-(1×1) units. We respectively replace one and five neighboring (1×1) Ge surface units so that 12.5% and 62.5% of the Ge(001)-(1×1) units are composed of the sixfold structures [Figs. 4(a) and 4(b)]. The computational procedures are the same as mentioned above. The calculated total energy differences are summarized in Table II with respect to the ratio of the sixfold coordination. The fully sixfold GeO₂/Ge interface is the most stable, and the mixed interface with the 12.5% sixfold structure is even more unstable than the fully fourfold GeO₂/Ge interface. The instabilities of the mixed interfaces are attributed to the grain boundaries; the *c*-axis of the fourfold oxidized region is more than 5% longer than that of the sixfold one. This result implies that the sixfold oxidized region exists as a large grain at the GeO₂/Ge interface.

Finally, we investigate the effect of the sixfold structure on the variations of the conduction band minimum (CBM) and VBM along the normal direction to the interface. To suppress the effect of quantum confinement due to the limitation of substrate thickness, a 12-atomic layer of the Ge(001) substrate is used. The four GeO₂ molecular layers are piled on the Ge(001) substrate, and other computational details are the same. It is believed that GeO₂ is composed of an amorphous structure. Tamura *et al.* found that the band gap of crystalline GeO₂ is compatible with that of amorphous GeO₂ by using the first-principles calculation [23]. Therefore, we calculate the electronic structure with and without a sixfold GeO₂ layer inserted between the crystalline fourfold GeO₂ layer and Ge(001) substrate. The grain boundary between the sixfold and fourfold structures parallel to the Ge(001) substrate is stable, although fivefold Ge atoms exist between the sixfold and fourfold boundaries. Figures 5(a) and 5(b) show the evolution of the CBM and VBM along a direction orthogonal to the interface plane, respectively. CBM and VBM variations are subtracted from the local density of states, calculated by integrating them on the plane parallel to the interface based

on $\rho(z, E) = \int |\psi(\mathbf{r}, E)|^2 d\mathbf{r}_{||}$, with a contour of $7.94 \times 10^{-5} \text{ e/eV/\AA}^3$. With the fourfold GeO₂/Ge interface, the VBM is almost complete at about 5 Å deep from the interface, which is similar than that with the SiO₂/Si interface [24], while the CBM saturates within 2 Å. Since the band gap of sixfold GeO₂ is narrower than that of fourfold GeO₂ [25], the valence electrons in the Ge substrate penetrate sixfold GeO₂ and the interface dipole emerges. Therefore, the existence of the sixfold GeO₂ layer shifts the VBM far from the interface toward the conduction band.

In summary, we proposed a sixfold GeO₂/Ge interface, in which the lattice mismatch at the interface is very small ($\sim 5\%$) and which is energetically much more stable than fourfold GeO₂/Ge interfaces. It should be noted that the sixfold structure was found to be a large grain at the GeO₂/Ge interface after computing the stability of the mixed fourfold and sixfold GeO₂/Ge interface. On the other hand, with SiO₂, a conventional fourfold structure on the Si(001) substrate is preferable due to the difficulty in rearranging the rigid O-Si-O bonds even in the bulk phase. The electronic structure calculation with and without the sixfold GeO₂ monolayer at the GeO₂/Ge interface reveals that the VBM far from the interface in the ultrathin GeO₂ layer ($\sim 10 \text{ Å}$) depends on the coordination number of GeO₂. Our results provide new insight into a strong candidate of the atomic and electronic structures of the GeO₂/Ge interface. We await experimental verification of our prediction.

The authors would like to thank Professor Kenji Shiraishi of University of Tsukuba, and Professor Heiji Watanabe, Professor Yoshitada Morikawa, Professor Takayoshi Shimura, and Professor Takuji Hosoi of Osaka University for reading the manuscript and for contributing to our fruitful discussions. This research was partially supported by the Strategic Japanese-German Cooperative Program from the Japan Science and Technology Agency and Deutsche Forschungsgemeinschaft, by a Grant-in-Aid for Young Scientists (B) (Grant No. 20710078), and also by a Grant-in-Aid for the Global COE "Center of Excellence for Atomically Controlled Fabrication Technology" from the Ministry of Education, Culture, Sports, Science and Technology, Japan. The numerical calculations were carried out using the computer facilities of the Institute for Solid State Physics at the University of Tokyo, the Center for Computational Sciences at University of Tsukuba, the Research Center for Computational Science at the National Institute of Natural Science, and the Information Synergy Center

at Tohoku University.

- [1] H. Matsubara, T. Sasada, M. Takenaka, and S. Takagi, Appl. Phys. Lett. **93**, 032104 (2008).
- [2] T. Hosoi, K. Kutsuki, G. Okamoto, M. Saito, T. Shimura, and H. Watanabe, Appl. Phys. Lett. **94**, 202112 (2009).
- [3] T. Maeda, T. Yasuda, M. Nishizawa, N. Miyata, Y. Morita, and S. Takagi, Appl. Phys. Lett. **85**, 3181 (2004).
- [4] V.V. Afanas'ev, Y.G. Fedorenko, and A. Stesmans, Appl. Phys. Lett. **87**, 032107 (2005).
- [5] A. Delabie, F. Bellenger, M. Houssa, T. Conard, S. Van Elshocht, M. Caymax, M. Heyns, and M. Meuris, Appl. Phys. Lett. **91**, 082904 (2007).
- [6] S. Takagi, T. Maeda, N. Taoka, M. Nishizawa, Y. Morita, K. Ikeda, Y. Yamashita, M. Nishikawa, H. Kumagai, R. Nakane, S. Sugahara, and N. Sugiyama, Microelect. Eng. **84**, 2314 (2007).
- [7] M. Houssa, G. Pourtois, M. Caymax, M. Meuris, M.M. Heyns, V.V. Afanas'ev, and A. Stesmans, Appl. Phys. Lett. **93**, 161909 (2008).
- [8] H. Kageshima and K. Shiraishi, Phys. Rev. Lett. **81**, 5936 (1998).
- [9] S. Saito, T. Hosoi, H. Watanabe, and T. Ono, Appl. Phys. Lett. **95**, 011908 (2009).
- [10] T. Watanabe, T. Onda, and I. Ohdomari, ECS Trans. **33**, 901 (2010).
- [11] M. Yang, R.Q. Wu, Q. Chen, W.S. Deng, Y.P. Feng, J.W. Chai, J.S. Pan, and S.J. Wang, Appl. Phys. Lett. **94**, 142903 (2009).
- [12] J.F. Binder, P. Broqvist, and A. Pasquarello, Microelect. Eng. **86**, 1760 (2009).
- [13] P. Broqvist, J.F. Binder, and A. Pasquarello, Appl. Phys. Lett. **94**, 141911 (2009).
- [14] M. Houssa, E.A. Chagarov and A.C. Kummel, MRS Bulletin **34**, 504 (2009).
- [15] L. Tsetseris and S.T. Pantelides, Appl. Phys. Lett. **95**, 262107 (2009).
- [16] J.R. Chelikowsky, N. Troullier, and Y. Saad, Phys. Rev. Lett. **72**, 1240 (1994); J.R. Chelikowsky, N. Troullier, K. Wu, and Y. Saad, Phys. Rev. B **50**, 11355 (1994).
- [17] K. Hirose, T. Ono, Y. Fujimoto, and S. Tsukamoto, *First-Principles Calculations in Real-Space Formalism, Electronic Configurations and Transport Properties of Nanostructures* (Imperial College, London, 2005).
- [18] T. Ono and K. Hirose, Phys. Rev. Lett. **82**, 5016 (1999); Phys. Rev. B **72**, 085115 (2005).

- 188 [19] We used the norm-conserving pseudopotentials NCPS97 constructed by K. Kobayashi; see K.
189 Kobayashi, Comput. Mater. Sci. **14**, 72 (1999).
- 190 [20] N. Troullier and J.L. Martins, Phys. Rev. B **43**, 1993 (1991).
- 191 [21] L. Kleinman and D.M. Bylander, Phys. Rev. Lett. **48**, 1425 (1982).
- 192 [22] J.P. Perdew and A. Zunger, Phys. Rev. B **23**, 5048 (1981).
- 193 [23] T. Tamura, G-H. Lu, R. Yamamoto, and M. Kohyama, Phys. Rev. B **69**, 195204 (2004).
- 194 [24] T. Yamasaki, C. Kaneta, T. Uchiyama, T. Uda, and K. Terakura, Phys. Rev. B **63**, 115314
195 (2001).
- 196 [25] The band gap of ~ 2.0 eV (~ 3.2 eV) is estimated for the sixfold (fourfold) GeO₂ at the local
197 density approximation level.

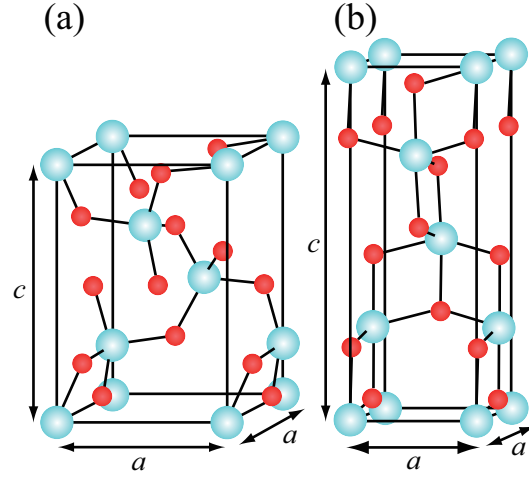


FIG. 1. (Color online) Unit cells of (a) fourfold and (b) sixfold c -GeO₂. The solid cube represents the unit-cell volume, and the blue (light) and red (dark) circles are Ge and O atoms, respectively.

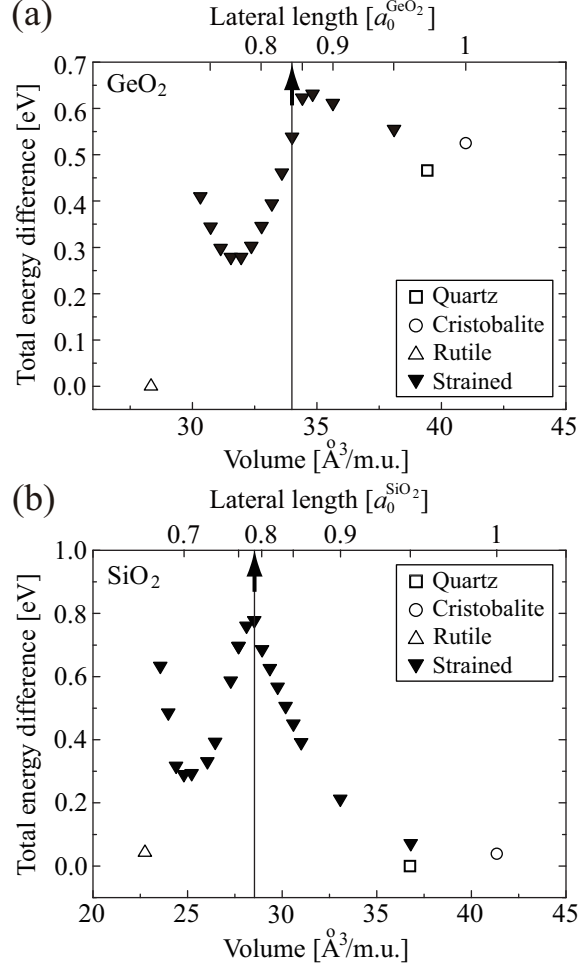


FIG. 2. Total energy per molecular unit (m.u.) as a function of volume for (a) c - GeO_2 and (b) SiO_2 . Energy minima of other phases [quartz (\square), cristobalite (\circ), and rutile (\triangle)] are also shown for comparison. The zero on the energy scale is rutile for GeO_2 and quartz for SiO_2 . The upper horizontal axes correspond to the lateral lengths of Ge and Si(001)-(1×1) surfaces in $a_0^{\text{GeO}_2}$ and $a_0^{\text{SiO}_2}$, where $a_0^{\text{GeO}_2}$ and $a_0^{\text{SiO}_2}$ represent the lengths of the a -axes of c - GeO_2 and c - SiO_2 at the equilibrium points, respectively.

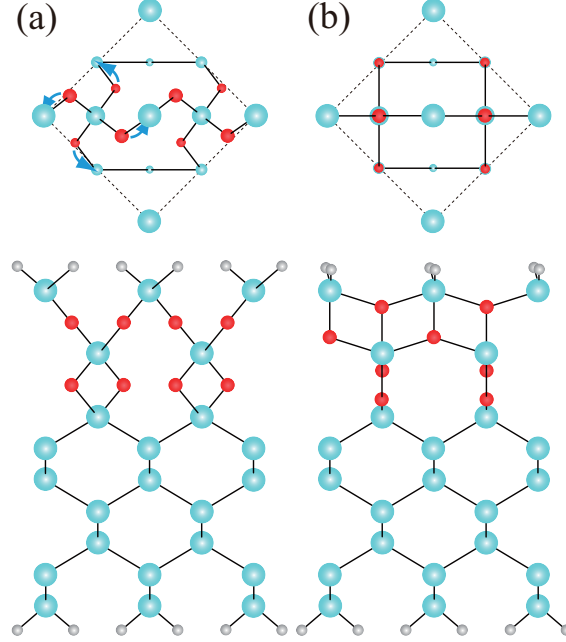


FIG. 3. (Color online) Top views and side views of (a) fourfold and (b) sixfold $\text{GeO}_2/\text{Ge}(001)$ interfaces. The blue (light), red (dark), and grey (light small) circles are Ge, O, and H atoms, respectively. The dotted square in the top views represents a $\text{Ge}(001)-(\sqrt{2} \times \sqrt{2})$ surface unit and the arrows indicate rotational directions to transform into sixfold structures.

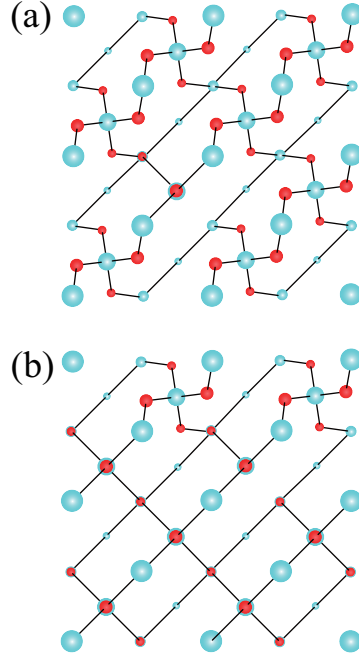


FIG. 4. (Color online) Top views of mixed fourfold and sixfold structures. (a) 12.5% and (b) 62.5% of Ge(001)-(1×1) surface units are composed of the sixfold structures. The blue (light) and red (dark) circles are Ge and O atoms, respectively.

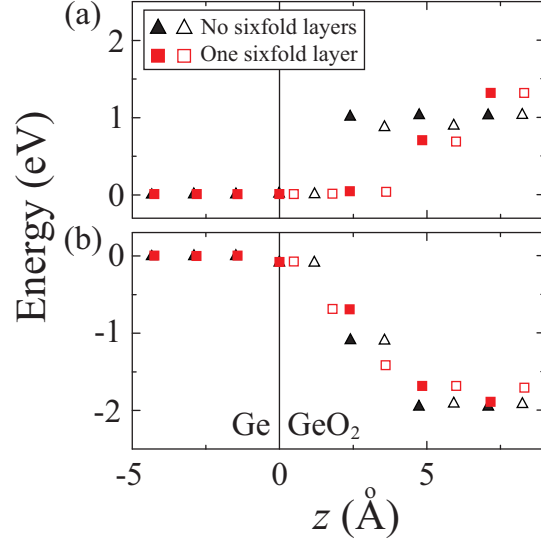


FIG. 5. (Color online) Variations of (a) CBM and (b) VBM along orthogonal direction to interface obtained on each atom. Triangles and squares are CBM and VBM of GeO_2/Ge interfaces with zero and one sixfold GeO_2 layers, respectively. Filled (open) symbols represent CBM and VBM on Ge (O) atoms. Solid line indicates boundary between GeO_2 and $\text{Ge}(001)$ substrate.

200

TABLES

201

TABLE I. Lattice constants of c -GeO₂ and c -SiO₂ at their equilibrium points. The unit is Å

Structure	a	c
c -GeO ₂	4.818	7.128
c -SiO ₂	4.925	6.828

TABLE II. Energy difference between fully fourfold c -GeO₂ structure and various mixing ratios of fourfold and sixfold structures with respect to ratio of sixfold structure. All units are in eV.

Ratio of sixfold structure	0%	12.5%	62.5%	100%
	0	0.92	-0.49	-7.67